2019

Proteomic analysis of Plasmodium falciparum histone deacetylase 1 complex proteins

Jessica A. Engel

Emma L. Norris

Paul Gilson

Jude Przyborski

Addmore Shonhai

See next page for additional authors

This article was originally published as:
Engel, J. A., Norris, E. L., Gilson, P., Przyborski, J., Shonhai, A., Blatch, G. L., Skinner, T. S., Gorman, J., Headlam, M., & Andrews, K. T. (2019). Proteomic analysis of Plasmodium falciparum histone deacetylase 1 complex proteins. *Experimental Parasitology, 198*, 7-16.

Original article available here:
10.1016/j.exppara.2019.01.008

This is the accepted manuscript version of an article published as:

Engel, J.A., Norris, E.L., Gibson, P., Przyborski, J., Shonhai, A., Blatch, G.L., Skinner-Adams, T.S., Gorman, J., Headlam, M., Andrews, K.T. (2019). Proteomic analysis of *Plasmodium falciparum* histone deacetylase 1 complex proteins. *Experimental Parasitology, 198,* 7-16. doi: 10.1016/j.exppara.2019.01.008

This article has been published in final form at https://doi.org/10.1016/j.exppara.2019.01.008

Proteomic analysis of *Plasmodium falciparum* histone deacetylase 1 complex proteins

Running title: Investigation of *Pf*HDAC1 complex proteins

Jessica A Engel[1], Emma L Norris[2], Paul Gilson[3], Jude Przyborski[4], Addmore Shonhai[5], Gregory L Blatch[6], Tina S Skinner-Adams[1], Jeffrey Gorman[2*], Madeleine Headlam[2*] and Katherine T Andrews[1#*]

[1]Griffith Institute for Drug Discovery, Griffith University, Queensland, Australia

[2]QIMR Berghofer Medical Research Institute, Queensland, Australia

[3]Burnet Institute, Monash University, Victoria, Australia

[4]Centre of Infectious Diseases, Parasitology, University Hospital Heidelberg, Germany

[5]Biochemistry Department, University of Venda, Thohoyandou, South Africa

[6]The Vice Chancellery, University of Notre Dame Australia, Fremantle, WA, Australia

*Co-senior authors

 # Corresponding author:

Professor KT Andrews, Griffith Institute for Drug Discovery, Don Young Road, Building N.75 Griffith University, Nathan, Queensland, Australia 4111; Ph ++61(0)7 3735 4420; Fax ++61(0)7 3735 6001; k.andrews@griffith.edu.au

Abstract

Plasmodium falciparum histone deacetylases (*Pf*HDACs) are an important class of epigenetic regulators that alter protein lysine acetylation, contributing to regulation of gene expression and normal parasite growth and development. *Pf*HDACs are therefore under investigation as drug targets for malaria. Despite this, our understanding of the biological roles of these enzymes is only just beginning to emerge. In higher eukaryotes, HDACs function as part of multi-protein complexes and act on both histone and non-histone substrates. Here, we present a proteomics analysis of *Pf*HDAC1 immunoprecipitates, identifying 26 putative *P. falciparum* complex proteins in trophozoite-stage asexual intraerythrocytic parasites. The co-migration of two of these (*P. falciparum* heat shock proteins 70-1 and 90) with *Pf*HDAC1 was validated using Blue Native PAGE combined with Western blot. These data provide a snapshot of possible *Pf*HDAC1 interactions and a starting point for future studies focused on elucidating the broader function of *Pf*HDACs in *Plasmodium* parasites.

Keywords: *Plasmodium falciparum*; malaria; histone deacetylase; immunoprecipitation; mass spectrometry; heat shock protein;

1. Introduction

Malaria causes substantial morbidity and mortality with 3.2 billion people at risk of infection globally. This results in more than 400,000 deaths each year, most due to infection with *Plasmodium falciparum* (WHO 2017). While the use of insecticide-treated bed nets, insecticide spraying, and the availability of drugs, including the gold standard artemisinin combination therapies (ACTs), has been responsible for a ~50% reduction in malaria associated deaths since 2000 (WHO 2017), malaria remains a serious health problem. A number of limitations still need to be overcome in order to achieve the global goal of malaria eradication. For instance, there is no highly effective malaria vaccine available, with the most advanced candidate (RTS,S) being only 30-40% effective in African children in phase III clinical trials (RTS 2015, RTS et al. 2012, RTS et al. 2011). In addition, almost all current antimalarial drugs, including ACTs, are now associated with resistance (Dondorp et al. 2010, Dondorp et al. 2009, WHO 2016). The potential loss of ACTs globally would be devastating (Burrows et al. 2014, malERA Consultative Group on Drugs 2011) and is driving discovery of new prevention and treatment strategies. An important part of the drug discovery process is understanding the biology of *Plasmodium* and the identification and validation of novel drug targets.

Plasmodium parasites undergo a number of developmental changes throughout their lifecycle that are governed by a tightly regulated cascade of gene expression (Bozdech et al. 2003). Epigenetic regulatory proteins, such as histone deacetylases (HDACs; also called lysine deacetylases), appear to play a key role in the regulation of this developmental cascade (Andrews et al. 2012, Chaal et al. 2010, Duraisingh and Horn 2016). HDACs, together with histone acetyltransferases (HATs), are involved in the reversible acetylation of histone and non-histone proteins in higher eukaryotes and the interplay between these two groups of enzymes results in changes to chromatin structure, gene expression and other cellular processes (Shahbazian and Grunstein 2007). As changes or mutations in human HDACs can contribute

to certain diseases such as cancer, there is increasing interest in therapeutic development of HDAC inhibitors (Cress and Seto 2000, Yang 2004), with some already clinically approved for various cancers (Garnock-Jones 2015, Grant et al. 2007, Prince and Dickinson 2012, Shi et al. 2015, Thompson 2014). HDACs are also showing promise as drug targets for several parasitic diseases, including malaria (Andrews et al. 2012, Andrews et al. 2012). Five HDAC homologues have been identified in the *P. falciparum* genome, fewer than in human cells where 18 HDACs are present (de Ruijter et al. 2003). HDACs can be grouped into four classes depending on their homology to a prototypical HDAC in yeast, co-factor dependency and subcellular localisation (de Ruijter et al. 2003, Haberland et al. 2009, Mariadason 2008). Class I HDACs are closely related to the transcriptional regulator RPD3 in the yeast *Saccharomyces cerevisiae*, whereas class II HDACs are related to the yeast HDA1 protein (de Ruijter et al. 2003, Gao et al. 2002). Class I and II HDACs are dependent on zinc as a co-factor for deacetylase activity (Mariadason 2008), while class III HDACs, also known as the silent information regulator 2 (Sir2)-related protein (sirtuin) HDAC family, are dependent on nicotinamide adenosine dinucleotide (NAD+) as a co-factor and are homologous to the yeast Sir2 gene (Gao et al. 2002, Mariadason 2008). *P. falciparum* HDAC (*Pf*HDAC) homologues are predicted to have homology to three human HDAC classes; class I (*Pf*HDAC1), class II (*Pf*HDAC2 and *Pf*HDAC3) and class III (*Pf*Sir2A and *Pf*Sir2B) (Andrews et al. 2012, Andrews et al. 2009, Horrocks et al. 2009). In *P. falciparum*, neither *Pf*Sir2A nor *Pf*Sir2B is essential in asexual intraerythrocytic stage parasites *in vitro,* but may play a role in parasite virulence (Duraisingh et al. 2005, Tonkin et al. 2009). The class I and II HDAC homologues are believed to be essential in the parasite (Coleman et al. 2014), making them potential antimalarial drug targets.

While it is known that HDACs from higher eukaryotes act as part of multi-protein complexes (de Ruijter et al. 2003, Kelly and Cowley 2013, Sengupta and Seto 2004), these complexes

have only been hypothesised via *in silico* analyses in *P. falciparum*, with no supporting experimental data (Goyal et al. 2012, Hernandez-Rivas et al. 2010, Horrocks et al. 2009, Merrick and Duraisingh 2007, Pallavi et al. 2010). Of the three class I and II *P. falciparum* HDAC homologues, only *Pf*HDAC1 has been functionally expressed *in vitro* (Patel et al. 2009), however nothing is known about its *in situ* function, including any dependence on accessory/complex proteins. Identifying *Pf*HDAC1 complex proteins could help elucidate the molecular function of this protein and also identify possible new drug targets in the form of non-histone substrates or proteins essential for *Pf*HDAC1 function. In this study, *Pf*HDAC1 was immunoprecipitated from native *P. falciparum* 3D7 protein lysates using an antibody raised against a C-terminal peptide of *Pf*HDAC1 and a proteomics analysis carried out in order to identify putative complex partners or substrates.

2. Materials and Methods

2.1 *Pf*HDAC1 antibody generation

Anti-*Pf*HDAC1 rabbit polyclonal antiserum was custom made (Innovative Veterinary Management System, Australia) against keyhole limpet hemocyanin-conjugated *Pf*HDAC1 C-terminal peptide RRKNYDDDFFDLSDRDQS (Mimotopes, Australia), using a previously reported peptide sequence (Joshi et al. 1999). Anti-*Pf*HDAC1 antibody was purified from sera using a Pierce™ Protein A Purification Kit (Thermo Fisher Scientific, Germany) and diluted in 50% glycerol prior to storage at -20°C.

2.2 *P. falciparum* protein lysate preparation

Synchronous *P. falciparum* 3D7 trophozoite-infected erythrocytes (5% hematocrit; 3-5% parasitemia) were pelleted by centrifugation and lysed with 0.15% saponin/phosphate buffered saline pH 7.4 (PBS). The resulting parasite pellet was washed extensively with PBS before

being resuspended in 10 volumes 1% Triton X-100/PBS containing cOmplete™ EDTA-free protease inhibitors (Roche, Germany). Following 30 min incubation on ice, with vortexing every 5 min, samples were centrifuged at 21,130 x *g* for 10 min at 4°C. Soluble protein in the supernatant was quantified using a Bradford Protein Assay kit (Bio-Rad, USA). Red blood cell control protein lysates were prepared as above with equivalent numbers of uninfected erythrocytes.

2.3 Immunoprecipitation and Western blot analysis

Indirect immunoprecipitation with anti-*Pf*HDAC1 antibody was carried out using a Dynabeads® Protein G Immunoprecipitation Kit (Life Technologies, USA) according to the manufacturer's protocol. Controls included a protein negative (PROT-NEG), antibody negative (AB-NEG), or red blood cell protein lysate (RBC) sample. Four independent experiments were performed. A portion of each protein sample (0.25 eluate volume) was separated by SDS-PAGE, followed by Western blot using different antibodies. The remaining sample of each eluate (0.75 eluate volume) was used for mass spectrometry analysis, as detailed in **Section 2.4**.

Primary antibodies used for Western blot analysis were anti-*Pf*HDAC1 rabbit antibody (1:5000 dilution), anti-*Pf*Hsp90 rabbit antibody (1:1000 dilution; **Supplementary Figure 1;** (Gitau et al. 2012)) and anti-*Pf*Hsp70-1 rabbit antibody (1:2000 dilution; **Supplementary Figure 1**; (Charnaud et al. 2017)). Anti-rabbit IgG light chain HRP mouse monoclonal SB62a secondary antibody (1:2000 dilution; Abcam, UK) was used for chemiluminescence detection on a VersaDoc 4000MP imaging system (Bio-Rad, USA). Secondary antibodies for fluorescence detection on an Odyssey FC (LI-COR Biosciences, USA) were anti-rabbit IRDye 800CW or anti-rabbit IRDye 680RD (LI-COR Biosciences, USA).

2.4 Protein reduction/alkylation and trypsin digestion

Samples were prepared for mass spectrometry analysis, as previously described (Hastie et al. 2012). Briefly, the samples were denatured with SDS, reduced with dithiothreitol, alkylated using iodoacetamide (IAA), and precipitated with 2 µl trypsin (0.5 µg/µl stock). The digested samples were then prepared for mass spectrometry analysis by acidification with formic acid (FA) at a 1% (v/v) final concentration.

2.5 Orbitrap mass spectrometry

The mass spectrometry experimental procedure used in this study was similar to that previously described (Dave et al. 2014). Tryptic digests were fractionated using a nanoAquity Ultra High Performance Liquid Chromatograph (nUHPLC; Waters, USA) with column equilibrated to 35ºC. The digests were loaded onto a Symmetry C18 100 Å, 180 µm x 20 mm trap (Waters, MA, USA) and washed at 15 µl/min in 1% acetonitrile containing 0.1% (v/v) formic acid for 3 min. Peptides were separated using a Peptide BEH C18 130 Å, 75 µm x 200 mm C18 column (Waters, MA, USA) at 35ºC using various gradients dependent on the samples analysed. A 90 min gradient and 1 µl injection volume was used for all samples originating from immunoprecipitations. Peptides were then analysed using an Orbitrap Velos Pro Mass Spectrometer. An electrospray ionisation source (Proxeon, Denmark) with a 10 µm inner diameter coated silica emitter (New Objective) introduced eluates from the separation column into an LTQ-Orbitrap Velos Pro (Thermo Fisher Scientific, Germany), which was controlled using Xcalibur 2.0 software (Thermo Fisher Scientific, Germany). The mass spectrometer was operated in a data-dependent mode to automatically switch between Orbitrap-MS and collision induced dissociated ion trap-MS/MS acquisition. Orbitrap resolution was set to 60,000 at m/z 400 and injection time was set to 200 ms and the top 15 MS peaks were fragmented and analysed by MS/MS per duty cycle.

2.6 Protein identification, quantification and functional annotation

158 Thermo Proteome Discoverer version 1.4.1.14 (Thermo Fisher Scientific, Germany) was used
159 to extract peak lists from Xcalibur raw files (parent ions in the mass range of 300-5000 *m/z*,
160 signal:noise ratio of 1.5). To identify human and *P. falciparum* proteins, Mascot version 2.5.1
161 (Matrix Science, UK) was used to search a concatenated database consisting of the complete
162 proteome sets for *H. sapiens* (73,540 canonical protein sequences downloaded from
163 www.uniprot.org on 7 December 2016) and *P. falciparum* 3D7 (5,548 protein sequences
164 downloaded from www.plasmodb.org on 7 December 2016). For the Mascot searches, the
165 fragment ion and parent ion mass tolerances were set to 0.8 Da and 20 ppm, respectively. Other
166 search parameters were trypsin enzyme digestion, a maximum of two missed cleavages, and
167 carbamidomethylation of cysteine was specified as a fixed modification. Protein N-terminal
168 acetylation, deamidation of asparagine/glutamine and methionine oxidation were specified as
169 variable modifications.

170 Scaffold™ version 4.5.3 (Proteome Software, USA) (Searle 2010) was used to validate and
171 quantify MS/MS-based peptide and protein identifications. Peptide identifications were
172 accepted if they were assigned a probability greater than 0.95 by the Scaffold legacy Peptide
173 Prophet algorithm (Keller et al. 2002). Protein identifications were accepted if they were
174 assigned a probability greater than 0.99 and contained at least two identified peptides. Protein
175 probabilities were assigned by the Protein Prophet algorithm (Nesvizhskii et al. 2003). Proteins
176 that contained similar peptides and could not be differentiated based on identified peptides
177 alone were grouped to satisfy the principles of parsimony.

178 Relative protein quantification was performed by spectral counting (Liu et al. 2004) using the
179 Scaffold reported exclusive spectrum counts. Protein groups quantified in at least three out of
180 four positive (*Pf*3D7) replicate samples were retained for statistical analysis. Statistical analysis
181 between the positive (*Pf*3D7-E) and negative (AB-NEG-E) replicate samples was carried out

using a beta-binomial test (Pham et al. 2010), where the total sample counts were set to the same value for all replicates (i.e., set to the average replicate total). The relative abundance of proteins in the *Pf*3D7 immunoprecipitations compared to the AB-NEG-E was estimated as a $\log_2$ fold-change calculated using $\log_2(\text{Avg}(Pf3D7\text{-}E) + 1) - \log_2(\text{Avg}(\text{AB-NEG-E}) + 1)$; a count of one was added to the average to allow calculation of fold-changes for protein groups not observed in the AB-NEG-E control. A significance level of $P \leq 0.01$ and a fold-change greater than two (i.e., a $\log_2$ fold-change greater than one) were applied to identify proteins that were enriched in the *Pf*3D7-E immunoprecipitation compared to the AB-NEG-E control.

Gene ontology (GO) annotations were downloaded from PlasmoDB (www.plasmodb.org on 20 January 2017; (Aurrecoechea et al. 2009)) and GOTermMapper (Boyle et al. 2004) for the proteins that were enriched in the *Pf*3D7 immunoprecipitation. The *P. falciparum* GeneDB GO Slim was used for GOTermMapper annotation.

2.7 Blue native polyacrylamide gel electrophoresis

Blue native polyacrylamide gel electrophoresis (BN PAGE) was carried out as previously described (Sessler et al. 2012), with the following modifications. Triton-X 100 (0.5%) detergent was used in the High Salt Lysis Buffer instead of 1% NP-40 and NativePAGE™ Novex® 3-12% Bis-Tris protein gels (Life Technologies, USA) were used for the separation of proteins. NativeMark™ unstained protein standard (Life Technologies, USA) was used as a molecular weight marker. Prior to Western blot, protein complexes were denatured by incubating the native gel in SDS PAGE Buffer (25 mM tris, 192 mM glycine, 0.1% SDS) for 10 min before transferring onto PVDF membrane (Merck Millipore, Germany). Second dimension SDS PAGE was performed as previously described (Elsworth et al. 2016) followed by colloidal Coomassie blue staining (Candiano et al. 2004) or Western blot analysis. For Western blot, membranes were probed sequentially following stripping in 25 mM glycine pH

2.0, 1% SDS and imaged on a VersaDoc 4000MP imaging system (Bio-Rad, USA) to confirm complete stripping. Image J 1.51d software was used to overlay Western blot images to determine co-localisation. For two dimensional BN PAGE/SDS PAGE, two colour Western blot analysis was carried out and membranes were subsequently imaged on an Odyssey Fc (LI-COR Biosciences, USA).

3. Results

3.1 Identification and functional annotation of *Pf*HDAC1 complex proteins

Prior to mass spectrometry analysis, Western blot was carried out on *P. falciparum* 3D7 trophozoite-stage protein lysates immunoprecipitated using anti-*Pf*HDAC1 antibody. A ~51 kDa protein, corresponding to the expected molecular mass of *Pf*HDAC1, was detected in the *Pf*3D7 starting material and *Pf*3D7 eluates for each of the four independent replicates (**Figure 1**; *Pf*3D7 lane SM and E, respectively). A background signal/smear observed in *Pf*3D7 samples was also seen in the eluates for the protein negative control (PROT-NEG-E) and RBC control (RBC-E) and is consistent with secondary antibody cross-reactivity to the *Pf*HDAC1 antibody heavy chain that is co-eluted with the target protein (Lal et al. 2005). Mass spectrometry analysis of immunoprecipitated material (*Pf*3D7-E and AB-NEG-E control) identified a total of 216 proteins, including 151 *P. falciparum* proteins and 65 human proteins (**Supplementary File 1**). Relative protein quantification was performed using spectral counting (Liu et al. 2004) and 135 proteins were quantified in the *Pf*3D7 immunoprecipitations (i.e. observed in at least three out of four replicate samples). To discriminate between candidate *Pf*HDAC1-binders and non-specific background, the abundance of proteins in the *Pf*3D7 immunoprecipitations was compared to the AB-NEG-E control using a beta-binomial test. Twenty-nine proteins were significantly enriched ($P<0.01$; >2-fold difference) in the *Pf*3D7 immunoprecipitation (**Table 1**; **Figure 2**). This included *Pf*HDAC1, 26 other *P. falciparum* proteins (**Table 1**) and two

Homo sapiens proteins (**Supplementary File 1**; highlighted in grey). The two human proteins, an uncharacterised protein (fragment; A0A0G2JRQ6) and immunoglobulin kappa variable 1-6 (fragment; IGKV1-6; A0A0C4DH72), both contain immunoglobulin-like domains (UniProt 2015) and are therefore most likely background signal from co-eluted antibody in the *Pf*3D7 eluate. As expected, *Pf*HDAC1 (PF3D7_0925700) was significantly enriched and had one of the largest fold-differences in the *Pf*3D7-E immunoprecipitation compared to the AB-NEG-E control ($P=7.1 \times 10^{-5}$, $\log_2$ fold-change=2.75), along with *Pf*Hsp70-1 (PF3D7_0818900; $P=2.1 \times 10^{-5}$; $\log_2$ fold-change=1.62) and *Pf*Hsp110 (PF3D7_0708800; $P=2.9 \times 10^{-5}$; $\log_2$ fold-change=2.52) (**Table 1**; **Figure 2)**. *Pf*Hsp90 (PF3D7_0708400) was also significantly enriched ($P=1.4 \times 10^{-3}$; $\log_2$ fold-change=1.10). Gene ontology annotations for the 26 candidate *Pf*HDAC1 complex proteins (from PlasmoDB) spanned 25 biological processes (**Figure 3** and **Supplementary File 1**). Eleven putative interactors were identified as having a role related to translation, the largest number of proteins in any one functional group.

3.2 Co-immunoprecipitation of putative *Pf*HDAC1 complex proteins.

Using antibodies available to putative complex members *Pf*Hsp70-1 and *Pf*Hsp90, Western blot analysis was carried out on *P. falciparum* 3D7 protein lysates immunoprecipitated with anti-*Pf*HDAC1 in order to confirm the immunoprecipitation-mass spectrometry data. As expected, the control Western blot with anti-*Pf*HDAC1 antibody detected a ~51 kDa band corresponding to *Pf*HDAC1 in the *Pf*3D7 starting material and *Pf*3D7 eluate samples (**Supplementary Figure 2**). This same blot was re-probed with anti-*Pf*Hsp70-1, which detected a band of the correct size of *Pf*Hsp70-1 (~74 kDa) in the starting material for the *Pf*3D7 and AB-NEG samples and in the *Pf*3D7 eluate, indicating that *Pf*Hsp70-1 co-immunoprecipitates with *Pf*HDAC1 (**Supplementary Figure 2**). While anti-*Pf*Hsp90 detected

253 a weak signal of the correct size (~86 kDa) in the *Pf*3D7 starting material and AB-NEG
254 samples, no signal was detected in the eluate material (not shown).

255 **3.3 Investigation of *Pf*HDAC1 protein interactions using BN PAGE analysis.**

256 Blue native PAGE, which allows detection of protein complexes using native polyacrylamide
257 gels (Camacho-Carvajal et al. 2004), was used in combination with Western blot to further
258 investigate *Pf*HDAC1 co-localisation with putative complex components in asexual stage *P.*
259 *falciparum* 3D7 parasites. Anti-*Pf*HDAC1 antibody resulted in prominent signals at ~200 kDa
260 and ~480 kDa in late trophozoites (LT; **Figure 4**), with relatively little to no signal observed
261 in the other developmental stages, whereas anti-*Pf*Hsp70-1 antibody resulted in prominent
262 signals at ~200 kDa, ~300 kDa and ~440 kDa in all four developmental stages (**Figure 4A**;
263 overexposed version shown in **Supplementary Figure 3**). Overlay of anti-*Pf*Hsp70-1 and anti-
264 *Pf*HDAC1 signals on the same membrane indicated possible co-migration of proteins at ~200
265 kDa in the LT sample (**Figure 4A**; **Merge**, arrow). Anti-*Pf*Hsp90 (**Figure 4B**) also detected
266 signals at ~200 kDa, ~300 kDa and ~440 kDa in the LT sample. Overlay of anti-*Pf*Hsp90 with
267 anti-*Pf*HDAC1 signal indicates that *Pf*HDAC1 and *Pf*Hsp90 putatively co-migrate at ~200 kDa
268 in the LT sample (**Figure 4B**; merge, arrow). When signals for anti-*Pf*Hsp70-1 and anti-
269 *Pf*Hsp90 were overlaid, putative co-migration for these proteins was observed at ~200 kDa,
270 ~300 kDa and ~440 kDa in the LT sample (**Figure 4C**; merge, arrows), in line with complex
271 sizes as previously identified in other studies for *Pf*Hsp70 and *Pf*Hsp90 (Banumathy et al. 2003,
272 Pavithra et al. 2004).

273

274 **3.4 Two dimensional BN PAGE / SDS PAGE analysis of *P. falciparum* protein lysates**

275 To further elucidate co-localisation of candidate *Pf*HDAC1 interacting proteins with
276 *Pf*HDAC1, protein complexes were separated by BN PAGE (**Figure 5A**), followed by

277 separation in a second dimension using SDS PAGE and colloidal Coomassie blue staining
278 (**Figure 5B**) or Western blot analysis (**Figure 5C**). The two-dimensional Western blot analyses
279 showed that *Pf*Hsp70-1 and *Pf*HDAC1 putatively co-occur within two protein complexes
280 (**Figure 5C**; panels *i* and *ii*) in *P. falciparum* 3D7 trophozoite-stage parasites. The protein
281 identity of the lower molecular weight signal recognised by the anti-*Pf*HDAC1 antibody at
282 ~40kDa is unknown and further validation using mass spectrometry is needed to confirm
283 whether this is a truncated form of *Pf*HDAC1 or a cross-reacting protein species.

284 **4. Discussion**

285 HDACs are regulators of *Plasmodium* transcription and play a role in lifecycle progression and
286 virulence gene expression (Andrews et al. 2012, Chaal et al. 2010, Duraisingh et al. 2005,
287 Merrick et al. 2012, Tonkin et al. 2009). This, together with several studies demonstrating that
288 certain HDAC inhibitors have potent *in vitro* activity against *P. falciparum* (IC_{50} <200 nM)
289 and parasite-specific selectivity (Selectivity Index >100) raises the possibility of developing
290 HDAC inhibitors as drug leads for malaria (Andrews et al. 2012, Chen et al. 2008, Hansen et
291 al. 2014, Patel et al. 2009, Patil et al. 2010). Therefore, gaining a better understanding of the
292 role that these proteins play in *Plasmodium* may lead to new insights to help facilitate research
293 in this area. In addition, identifying *Pf*HDAC complex proteins may not only yield new
294 mechanistic insights but could potentially identify new pathways associated with HDAC
295 action/function that could be therapeutic targets in the future.

296 In this study, *Pf*HDAC1 immunoprecipitation combined with mass spectrometry analysis
297 identified 26 putative *Pf*HDAC1 complex proteins in *P. falciparum* 3D7 trophozoite-stage
298 parasites (**Table 1**). In addition, and validating the immunoprecipitation, *Pf*HDAC1 was also
299 one of the top significantly enriched proteins present in the *Pf*3D7 immunoprecipitated material
300 (**Table 1**; $P=7 \times 10^{-5}$). In the context of the discussion below, it is important to remember that

the candidate *Pf*HDAC1 complex proteins identified in this study are likely to represent only a "snapshot" of the "*Pf*HDAC1 interactome", based on the experimental conditions used. *Pf*HDAC1 protein interactions are likely to be dynamic and transient as a result of the highly regulated cascade of gene expression that occurs across the asexual intraerythrocytic developmental cycle (Bozdech et al. 2003, Le Roch et al. 2003). In addition, some proteins identified may not necessarily be direct interactors of *Pf*HDAC1, but rather part of immunoprecipitated complexes.

Gene ontology annotations of the 26 *Pf*HDAC1 co-precipitated proteins span processes including translation, protein folding, glycolysis and others (**Figure 3**), indicating the potential diverse roles that *Pf*HDAC1 may play within the parasite, either directly or indirectly. When the proteins were annotated using broader, high-level GO biological process terms (Boyle et al. 2004, Princeton University) ten had the annotation "translation" (GO:0006412), including eight ribosomal proteins, elongation factor 2 (PF3D7_1451100) and asparagine-tRNA ligase (PF3D7_0211800) (**Supplementary Table 1** and **2**). Ribosomal proteins are often identified in *P. falciparum* immunoprecipitations (Dorin-Semblat et al. 2015, Russo et al. 2010) and so it is possible they may be non-specific interactors. However, there is evidence of HDAC association with ribosomal proteins. For example, human HDAC6 has been shown to be recruited to ribosomes and to regulate *de novo* protein translation in keratinocytes after arsenite stress (Kappeler et al. 2012). Furthermore lysine acetylation sites are present on ribosomal proteins from humans (Choudhary et al. 2009) and *Plasmodium* (Cobbold et al. 2016). Lysine acetylation marks are also present on the putative *Pf*HDAC interacting proteins *P. falciparum* elongation factor 2 and asparagine-tRNA ligase (Cobbold et al. 2016) and, in human cells, translational elongation factors have been associated with HDACs/HDAC inhibition (Alam et al. 2016, Greer et al. 2015).

Four heat shock proteins (Hsp's) were among the putative *Pf*HDAC1 interacting proteins identified in this study - *Pf*Hsp70-1, *Pf*Hsp110, *Pf*Hsp90 and *Pf*Hsp60. Interestingly, *Pf*Hsp70-1, *Pf*Hsp110 and *Pf*Hsp90 were previously predicted to interact with *Pf*HDAC1 in an *in silico* study (Pavithra et al. 2007) that utilized human protein interaction predictions from the Human Protein Reference Database (HPRD) and *P. falciparum* yeast-two-hybrid data (LaCount et al. 2005, Pavithra et al. 2007). *Pf*Hsp110 is likely a nucleotide exchange factor for *Pf*Hsp70-1 and thus may be an indirect immunoprecipitate in our study (Zininga et al. 2016). A study using antibodies specific for human HDAC1, HDAC2 and HDAC3 has shown that these proteins co-immunoprecipitate with human Hsp70 (*Hs*Hsp70) (Johnson et al. 2002). In HeLa nuclear extracts, an interaction between *Hs*HDAC3 and *Hs*Hsp70 has also been confirmed using mass spectrometry (Yoon et al. 2003). Furthermore, HDACs have been shown to associate with Hsp70-like proteins in the closely related apicomplexan parasite *Toxoplasma gondii* (Saksouk et al. 2005). *Tg*HDAC3 (class I HDAC) associates with *Tg*Hsp70a (TGME49_311720; chaperone protein BiP) and *Tg*Hsp70b (TGME49_273760) (Saksouk et al. 2005). Of the six putative HDACs identified in *T. gondii*, *Tg*HDAC3 has highest sequence similarity to *Pf*HDAC1 (Aurrecoechea et al. 2009). *Tg*Hsp70b has greatest sequence similarity to *Pf*Hsp70-1, as determined by BLASTp analysis (Aurrecoechea et al. 2009). Interestingly, a Hsp90-like protein (TGME49_244560) was also identified as a *Tg*HDAC3 complex constituent in the same study. Other evidence for HDAC interaction with Hsp's includes a study showing that human Hsp90 activity is regulated by reversible acetylation through interaction with *Hs*HDAC6 (Kovacs et al. 2005). In *P. falciparum*, a potential although indirect association of a *Pf*HDAC protein (isoform not identified) with *Pf*Hsp90-containing complexes has also been reported (Pallavi et al. 2010). Furthermore, multiple acetyl-lysine sites have been identified on *P. falciparum* heat shock proteins indicating possible regulation of these proteins through acetylation (Cobbold et al. 2016, Miao et al. 2013).

Our preliminary validation data focused on candidate *Pf*HDAC1 complex proteins *Pf*Hsp70-1 and *Pf*Hsp90. These proteins were selected based on the literature evidence for interactions with HDACs, as discussed above, and the availability of validated antibodies to these proteins. Western blot data on *Pf*HDAC1 immunoprecipitation eluates indicated that *Pf*Hsp70-1 is co-immunoprecipitated with *Pf*HDAC1. However, this approach did not detect co-immunoprecipitation of *Pf*Hsp90, possibly due to low abundance of this protein in the starting material. In a second approach combining BN PAGE and Western blot, *Pf*HDAC1 co-occurred with *Pf*Hsp70-1 and *Pf*Hsp90 in trophozoite-stage samples. These data indicate that *Pf*Hsp90 (~86 kDa) and *Pf*Hsp70-1 (~74 kDa) putatively co-occur with *Pf*HDAC1 (~51 kDa) in a ~200-250 kDa complex (**Figure 4**). While this complex size is somewhat smaller than might be predicted given that *Pf*Hsp90 normally exists as a dimer (Corbett and Berger 2010, Pallavi et al. 2010), we cannot rule out dimer dissociation due to the triton-X-100 concentration used, as has been previously seen in other studies (Fiala et al. 2011). In an independent validation method, 2D-PAGE analysis of *P. falciparum* trophozoite-stage protein lysates indicated that *Pf*Hsp70-1 co-occurs with *Pf*HDAC1 in two distinct complexes, further validating this interaction.

It has been proposed that HDAC proteins possess glutamine-rich domains, and as a result of hydrophobic patches, do not fold stably (Guo et al. 2007). This could be why *Pf*HDAC1 is recognized by molecular chaperones such as *Pf*Hsp70-1 and *Pf*Hsp90. Thus, it may also be that *Pf*HDAC1 acts as a substrate, rather than a partner protein, for *Pf*Hsp70-1 and *Pf*Hsp90. Both *Pf*Hsp70-1 and *Pf*Hsp90 are potential anti-plasmodial drug targets that have been investigated *in vitro*, and *in vivo* (Cockburn et al. 2014, Cockburn et al. 2011, Mout et al. 2012, Murillo-Solano et al. 2017, Pallavi et al. 2010, Pesce et al. 2010, Shonhai 2010, Wang et al. 2014, Wang et al. 2016, Zininga et al. 2017). The majority of studies have focused on identifying *Pf*Hsp90 inhibitors (Murillo-Solano et al. 2017, Pallavi et al. 2010, Posfai et al. 2018, Wang et al. 2014,

Wang et al. 2016) as this protein is essential for *P. falciparum* growth and development (Banumathy et al. 2003). However, heat shock proteins are highly conserved between species and therefore the selectivity of *Pf*Hsp inhibitors for parasite protein versus human orthologues has been problematically low. With the identification of structural differences between the parasite and human Hsp's, as carried out by Wang et al. (Wang et al. 2014) for *Pf*Hsp90, the development of *Plasmodium*-specific heat shock protein inhibitors is theoretically possible. The data presented in this study, suggests it would be of interest to examine the efficacy of combination therapies containing Hsp90, Hsp70-1 and HDAC inhibitors to determine if such a combination strategy may result in improved efficacy of these compounds. Pallavi et al. have previously shown an additive and synergistic interaction between geldanamycin (Hsp90 inhibitor) and Trichostatin A (TSA; pan-HDAC inhibitor) in inhibiting *P. falciparum* growth (Pallavi et al. 2010). Future studies could investigate interactions between class I specific-HDAC inhibitors and recently identified *Pf*Hsp90 or *Pf*Hsp70 inhibitors.

In summary, this is the first study to investigate *Pf*HDAC1 complex proteins in *P. falciparum.* A set of 26 candidate *Pf*HDAC1 interacting proteins were identified in saponin-lysed trophozoite-stage *P. falciparum* 3D7 parasites, and the association of two (*Pf*Hsp70-1 and *Pf*Hsp90) further investigated using independent methods. These data contribute to our understanding of the function of *Pf*HDAC1 within asexual stage malaria parasites. Furthermore, these findings provide a platform for future studies focused on elucidating the broader function of *Pf*HDACs in *Plasmodium* and the investigation of their interacting proteins, including temporal changes over the course of the intra-erythrocytic life-cycle.

Acknowledgements

We thank Griffith University for scholarship support (GUIPRS and GUPRS to JAE). Access to proteomic infrastructure in the QIMR Berghofer Protein Discovery Centre was made possible by funding from Bioplatforms Australia and the Queensland State Government provided through the Australian Government National Collaborative Infrastructure Strategy (NCRIS) and EIF Fund. We thank the Australian Red Cross Blood Service for the provision of human blood and sera.

References

Alam, N., L. Zimmerman, N. A. Wolfson, C. G. Joseph, C. A. Fierke and O. Schueler-Furman (2016). Structure-Based Identification of HDAC8 Non-histone Substrates. Structure 24(3): 458-468.

Andrews, K. T., A. P. Gupta, T. N. Tran, D. P. Fairlie, G. N. Gobert and Z. Bozdech (2012). Comparative gene expression profiling of *P. falciparum* malaria parasites exposed to three different histone deacetylase inhibitors. PLoS One 7(2): e31847.

Andrews, K. T., A. Haque and M. K. Jones (2012). HDAC inhibitors in parasitic diseases. Immunol Cell Biol 90(1): 66-77.

Andrews, K. T., T. N. Tran and D. P. Fairlie (2012). Towards histone deacetylase inhibitors as new antimalarial drugs. Curr Pharm Des 18(24): 3467-3479.

Andrews, K. T., T. N. Tran, N. C. Wheatley and D. P. Fairlie (2009). Targeting histone deacetylase inhibitors for anti-malarial therapy. Curr Top Med Chem 9(3): 292-308.

Aurrecoechea, C., J. Brestelli, B. P. Brunk, J. Dommer, S. Fischer, B. Gajria, X. Gao, A. Gingle, G. Grant, O. S. Harb, M. Heiges, F. Innamorato, J. Iodice, J. C. Kissinger, E. Kraemer, W. Li, J. A. Miller, V. Nayak, C. Pennington, D. F. Pinney, D. S. Roos, C. Ross, C. J. Stoeckert, Jr., C. Treatman and H. Wang (2009). PlasmoDB: a functional genomic database for malaria parasites. Nucleic Acids Res 37(Database issue): D539-543.

Banumathy, G., V. Singh, S. R. Pavithra and U. Tatu (2003). Heat shock protein 90 function is essential for *Plasmodium falciparum* growth in human erythrocytes. J Biol Chem 278(20): 18336-18345.

Boyle, E. I., S. Weng, J. Gollub, H. Jin, D. Botstein, J. M. Cherry and G. Sherlock (2004). GO::TermFinder--open source software for accessing Gene Ontology information and finding significantly enriched Gene Ontology terms associated with a list of genes. Bioinformatics 20(18): 3710-3715.

Bozdech, Z., M. Llinas, B. L. Pulliam, E. D. Wong, J. Zhu and J. L. DeRisi (2003). The transcriptome of the intraerythrocytic developmental cycle of *Plasmodium falciparum*. PLoS Biol 1(1): E5.

Burrows, J. N., E. Burlot, B. Campo, S. Cherbuin, S. Jeanneret, D. Leroy, T. Spangenberg, D. Waterson, T. N. Wells and P. Willis (2014). Antimalarial drug discovery - the path towards eradication. Parasitology 141(1): 128-139.

Camacho-Carvajal, M. M., B. Wollscheid, R. Aebersold, V. Steimle and W. W. Schamel (2004). Two-dimensional Blue native/SDS gel electrophoresis of multi-protein complexes from whole cellular lysates: a proteomics approach. Mol Cell Proteomics 3(2): 176-182.

Candiano, G., M. Bruschi, L. Musante, L. Santucci, G. M. Ghiggeri, B. Carnemolla, P. Orecchia, L. Zardi and P. G. Righetti (2004). Blue silver: a very sensitive colloidal Coomassie G-250 staining for proteome analysis. Electrophoresis 25(9): 1327-1333.
Chaal, B. K., A. P. Gupta, B. D. Wastuwidyaningtyas, Y. H. Luah and Z. Bozdech (2010). Histone deacetylases play a major role in the transcriptional regulation of the *Plasmodium falciparum* life cycle. PLoS Pathog 6(1): e1000737.
Charnaud, S. C., M. W. A. Dixon, C. Q. Nie, L. Chappell, P. R. Sanders, T. Nebl, E. Hanssen, M. Berriman, J. A. Chan, A. J. Blanch, J. G. Beeson, J. C. Rayner, J. M. Przyborski, L. Tilley, B. S. Crabb and P. R. Gilson (2017). The exported chaperone Hsp70-x supports virulence functions for Plasmodium falciparum blood stage parasites. PLoS One 12(7): e0181656.
Chen, Y., M. Lopez-Sanchez, D. N. Savoy, D. D. Billadeau, G. S. Dow and A. P. Kozikowski (2008). A series of potent and selective, triazolylphenyl-based histone deacetylases inhibitors with activity against pancreatic cancer cells and *Plasmodium falciparum*. Journal of Medicinal Chemistry 51(12): 3437-3448.
Choudhary, C., C. Kumar, F. Gnad, M. L. Nielsen, M. Rehman, T. C. Walther, J. V. Olsen and M. Mann (2009). Lysine acetylation targets protein complexes and co-regulates major cellular functions. Science 325(5942): 834-840.
Cobbold, S. A., J. M. Santos, A. Ochoa, D. H. Perlman and M. Llinas (2016). Proteome-wide analysis reveals widespread lysine acetylation of major protein complexes in the malaria parasite. Sci Rep 6: 19722.
Cockburn, I. L., A. Boshoff, E. R. Pesce and G. L. Blatch (2014). Selective modulation of plasmodial Hsp70s by small molecules with antimalarial activity. Biol Chem 395(11): 1353-1362.
Cockburn, I. L., E. R. Pesce, J. M. Pryzborski, M. T. Davies-Coleman, P. G. Clark, R. A. Keyzers, L. L. Stephens and G. L. Blatch (2011). Screening for small molecule modulators of Hsp70 chaperone activity using protein aggregation suppression assays: inhibition of the plasmodial chaperone PfHsp70-1. Biol Chem 392(5): 431-438.
Coleman, B. I., K. M. Skillman, R. H. Jiang, L. M. Childs, L. M. Altenhofen, M. Ganter, Y. Leung, I. Goldowitz, B. F. Kafsack, M. Marti, M. Llinas, C. O. Buckee and M. T. Duraisingh (2014). A *Plasmodium falciparum* histone deacetylase regulates antigenic variation and gametocyte conversion. Cell Host Microbe 16(2): 177-186.
Corbett, K. D. and J. M. Berger (2010). Structure of the ATP-binding domain of Plasmodium falciparum Hsp90. Proteins 78(13): 2738-2744.
Cress, W. D. and E. Seto (2000). Histone deacetylases, transcriptional control, and cancer. J Cell Physiol 184(1): 1-16.
Dave, K. A., E. L. Norris, A. A. Bukreyev, M. J. Headlam, U. J. Buchholz, T. Singh, P. L. Collins and J. J. Gorman (2014). A comprehensive proteomic view of responses of A549 type II alveolar epithelial cells to human respiratory syncytial virus infection. Mol Cell Proteomics 13(12): 3250-3269.
de Ruijter, A. J., A. H. van Gennip, H. N. Caron, S. Kemp and A. B. van Kuilenburg (2003). Histone deacetylases (HDACs): characterization of the classical HDAC family. Biochem J 370(Pt 3): 737-749.
Dondorp, A. M., C. I. Fanello, I. C. Hendriksen, E. Gomes, A. Seni, K. D. Chhaganlal, K. Bojang, R. Olaosebikan, N. Anunobi, K. Maitland, E. Kivaya, T. Agbenyega, S. B. Nguah, J. Evans, S. Gesase, C. Kahabuka, G. Mtove, B. Nadjm, J. Deen, J. Mwanga-Amumpaire, M. Nansumba, C. Karema, N. Umulisa, A. Uwimana, O. A. Mokuolu, O. T. Adedoyin, W. B. Johnson, A. K. Tshefu, M. A. Onyamboko, T. Sakulthaew, W. P. Ngum, K. Silamut, K. Stepniewska, C. J. Woodrow, D. Bethell, B. Wills, M. Oneko, T. E. Peto, L. von Seidlein, N. P. Day, N. J. White and A. group (2010). Artesunate versus

quinine in the treatment of severe falciparum malaria in African children (AQUAMAT): an open-label, randomised trial. Lancet 376(9753): 1647-1657.
Dondorp, A. M., F. Nosten, P. Yi, D. Das, A. P. Phyo, J. Tarning, K. M. Lwin, F. Ariey, W. Hanpithakpong, S. J. Lee, P. Ringwald, K. Silamut, M. Imwong, K. Chotivanich, P. Lim, T. Herdman, S. S. An, S. Yeung, P. Singhasivanon, N. P. Day, N. Lindegardh, D. Socheat and N. J. White (2009). Artemisinin resistance in *Plasmodium falciparum* malaria. N Engl J Med 361(5): 455-467.
Dorin-Semblat, D., C. Demarta-Gatsi, R. Hamelin, F. Armand, T. G. Carvalho, M. Moniatte and C. Doerig (2015). Malaria Parasite-Infected Erythrocytes Secrete PfCK1, the *Plasmodium* Homologue of the Pleiotropic Protein Kinase Casein Kinase 1. PLoS One 10(12): e0139591.
Duraisingh, M. T. and D. Horn (2016). Epigenetic Regulation of Virulence Gene Expression in Parasitic Protozoa. Cell Host Microbe 19(5): 629-640.
Duraisingh, M. T., T. S. Voss, A. J. Marty, M. F. Duffy, R. T. Good, J. K. Thompson, L. H. Freitas-Junior, A. Scherf, B. S. Crabb and A. F. Cowman (2005). Heterochromatin silencing and locus repositioning linked to regulation of virulence genes in *Plasmodium falciparum*. Cell 121(1): 13-24.
Elsworth, B., P. R. Sanders, T. Nebl, S. Batinovic, M. Kalanon, C. Q. Nie, S. C. Charnaud, H. E. Bullen, T. F. de Koning Ward, L. Tilley, B. S. Crabb and P. R. Gilson (2016). Proteomic analysis reveals novel proteins associated with the *Plasmodium* protein exporter PTEX and a loss of complex stability upon truncation of the core PTEX component, PTEX150. Cell Microbiol.
Fiala, G. J., W. W. Schamel and B. Blumenthal (2011). Blue native polyacrylamide gel electrophoresis (BN-PAGE) for analysis of multiprotein complexes from cellular lysates. J Vis Exp(48).
Gao, L., M. A. Cueto, F. Asselbergs and P. Atadja (2002). Cloning and functional characterization of HDAC11, a novel member of the human histone deacetylase family. J Biol Chem 277(28): 25748-25755.
Garnock-Jones, K. P. (2015). Panobinostat: first global approval. Drugs 75(6): 695-704.
Gitau, G. W., P. Mandal, G. L. Blatch, J. Przyborski and A. Shonhai (2012). Characterisation of the *Plasmodium falciparum* Hsp70-Hsp90 organising protein (*Pf*Hop). Cell Stress Chaperones 17(2): 191-202.
Goyal, M., A. Alam, M. S. Iqbal, S. Dey, S. Bindu, C. Pal, A. Banerjee, S. Chakrabarti and U. Bandyopadhyay (2012). Identification and molecular characterization of an Alba-family protein from human malaria parasite Plasmodium falciparum. Nucleic Acids Res 40(3): 1174-1190.
Grant, S., C. Easley and P. Kirkpatrick (2007). Vorinostat. Nat Rev Drug Discov 6(1): 21-22.
Greer, C. B., Y. Tanaka, Y. J. Kim, P. Xie, M. Q. Zhang, I. H. Park and T. H. Kim (2015). Histone Deacetylases Positively Regulate Transcription through the Elongation Machinery. Cell Rep 13(7): 1444-1455.
Guo, L., A. Han, D. L. Bates, J. Cao and L. Chen (2007). Crystal structure of a conserved N-terminal domain of histone deacetylase 4 reveals functional insights into glutamine-rich domains. Proc Natl Acad Sci U S A 104(11): 4297-4302.
Haberland, M., R. L. Montgomery and E. N. Olson (2009). The many roles of histone deacetylases in development and physiology: implications for disease and therapy. Nat Rev Genet 10(1): 32-42.
Hansen, F. K., S. D. Sumanadasa, K. Stenzel, S. Duffy, S. Meister, L. Marek, R. Schmetter, K. Kuna, A. Hamacher, B. Mordmuller, M. U. Kassack, E. A. Winzeler, V.

M. Avery, K. T. Andrews and T. Kurz (2014). Discovery of HDAC inhibitors with potent activity against multiple malaria parasite life cycle stages. Eur J Med Chem 82: 204-213.
Hastie, M. L., M. J. Headlam, N. B. Patel, A. A. Bukreyev, U. J. Buchholz, K. A. Dave, E. L. Norris, C. L. Wright, K. M. Spann, P. L. Collins and J. J. Gorman (2012). The human respiratory syncytial virus nonstructural protein 1 regulates type I and type II interferon pathways. Mol Cell Proteomics 11(5): 108-127.
Hernandez-Rivas, R., K. Perez-Toledo, A. M. Herrera Solorio, D. M. Delgadillo and M. Vargas (2010). Telomeric heterochromatin in Plasmodium falciparum. J Biomed Biotechnol 2010: 290501.
Horrocks, P., E. Wong, K. Russell and R. D. Emes (2009). Control of gene expression in *Plasmodium falciparum* - ten years on. Mol Biochem Parasitol 164(1): 9-25.
Johnson, C. A., D. A. White, J. S. Lavender, L. P. O'Neill and B. M. Turner (2002). Human class I histone deacetylase complexes show enhanced catalytic activity in the presence of ATP and co-immunoprecipitate with the ATP-dependent chaperone protein Hsp70. J Biol Chem 277(11): 9590-9597.
Joshi, M. B., D. T. Lin, P. H. Chiang, N. D. Goldman, H. Fujioka, M. Aikawa and C. Syin (1999). Molecular cloning and nuclear localization of a histone deacetylase homologue in *Plasmodium falciparum*. Mol Biochem Parasitol 99(1): 11-19.
Kappeler, K. V., J. Zhang, T. N. Dinh, J. G. Strom and Q. M. Chen (2012). Histone deacetylase 6 associates with ribosomes and regulates de novo protein translation during arsenite stress. Toxicol Sci 127(1): 246-255.
Keller, A., A. I. Nesvizhskii, E. Kolker and R. Aebersold (2002). Empirical statistical model to estimate the accuracy of peptide identifications made by MS/MS and database search. Anal Chem 74(20): 5383-5392.
Kelly, R. D. and S. M. Cowley (2013). The physiological roles of histone deacetylase (HDAC) 1 and 2: complex co-stars with multiple leading parts. Biochem Soc Trans 41(3): 741-749.
Kovacs, J. J., P. J. Murphy, S. Gaillard, X. Zhao, J. T. Wu, C. V. Nicchitta, M. Yoshida, D. O. Toft, W. B. Pratt and T. P. Yao (2005). HDAC6 regulates Hsp90 acetylation and chaperone-dependent activation of glucocorticoid receptor. Mol Cell 18(5): 601-607.
LaCount, D. J., M. Vignali, R. Chettier, A. Phansalkar, R. Bell, J. R. Hesselberth, L. W. Schoenfeld, I. Ota, S. Sahasrabudhe, C. Kurschner, S. Fields and R. E. Hughes (2005). A protein interaction network of the malaria parasite *Plasmodium falciparum*. Nature 438(7064): 103-107.
Lal, A., S. R. Haynes and M. Gorospe (2005). Clean Western blot signals from immunoprecipitated samples. Mol Cell Probes 19(6): 385-388.
Le Roch, K. G., Y. Zhou, P. L. Blair, M. Grainger, J. K. Moch, J. D. Haynes, P. De La Vega, A. A. Holder, S. Batalov, D. J. Carucci and E. A. Winzeler (2003). Discovery of gene function by expression profiling of the malaria parasite life cycle. Science 301(5639): 1503-1508.
Liu, H., R. G. Sadygov and J. R. Yates, 3rd (2004). A model for random sampling and estimation of relative protein abundance in shotgun proteomics. Anal Chem 76(14): 4193-4201.
malERA Consultative Group on Drugs (2011). A research agenda for malaria eradication: drugs. PLoS Med 8(1): e1000402.
Mariadason, J. M. (2008). HDACs and HDAC inhibitors in colon cancer. Epigenetics 3(1): 28-37.
Merrick, C. J. and M. T. Duraisingh (2007). Plasmodium falciparum Sir2: an unusual sirtuin with dual histone deacetylase and ADP-ribosyltransferase activity. Eukaryot Cell 6(11): 2081-2091.

Merrick, C. J., C. Huttenhower, C. Buckee, A. Amambua-Ngwa, N. Gomez-Escobar, M. Walther, D. J. Conway and M. T. Duraisingh (2012). Epigenetic dysregulation of virulence gene expression in severe *Plasmodium falciparum* malaria. J Infect Dis 205(10): 1593-1600.
Miao, J., M. Lawrence, V. Jeffers, F. Zhao, D. Parker, Y. Ge, W. J. Sullivan, Jr. and L. Cui (2013). Extensive lysine acetylation occurs in evolutionarily conserved metabolic pathways and parasite-specific functions during *Plasmodium falciparum* intraerythrocytic development. Mol Microbiol 89(4): 660-675.
Mout, R., Z. D. Xu, A. K. Wolf, V. Jo Davisson and G. K. Jarori (2012). Anti-malarial activity of geldanamycin derivatives in mice infected with Plasmodium yoelii. Malar J 11: 54.
Murillo-Solano, C., C. Dong, C. G. Sanchez and J. C. Pizarro (2017). Identification and characterization of the antiplasmodial activity of Hsp90 inhibitors. Malar J 16(1): 292.
Nesvizhskii, A. I., A. Keller, E. Kolker and R. Aebersold (2003). A statistical model for identifying proteins by tandem mass spectrometry. Anal Chem 75(17): 4646-4658.
Pallavi, R., N. Roy, R. K. Nageshan, P. Talukdar, S. R. Pavithra, R. Reddy, S. Venketesh, R. Kumar, A. K. Gupta, R. K. Singh, S. C. Yadav and U. Tatu (2010). Heat shock protein 90 as a drug target against protozoan infections: biochemical characterization of HSP90 from *Plasmodium falciparum* and *Trypanosoma evansi* and evaluation of its inhibitor as a candidate drug. J Biol Chem 285(49): 37964-37975.
Patel, V., R. Mazitschek, B. Coleman, C. Nguyen, S. Urgaonkar, J. Cortese, R. H. Barker, E. Greenberg, W. Tang, J. E. Bradner, S. L. Schreiber, M. T. Duraisingh, D. F. Wirth and J. Clardy (2009). Identification and characterization of small molecule inhibitors of a class I histone deacetylase from *Plasmodium falciparum*. J Med Chem 52(8): 2185-2187.
Patil, V., W. Guerrant, P. C. Chen, B. Gryder, D. B. Benicewicz, S. I. Khan, B. L. Tekwani and A. K. Oyelere (2010). Antimalarial and antileishmanial activities of histone deacetylase inhibitors with triazole-linked cap group. Bioorg Med Chem 18(1): 415-425.
Pavithra, S. R., G. Banumathy, O. Joy, V. Singh and U. Tatu (2004). Recurrent fever promotes *Plasmodium falciparum* development in human erythrocytes. J Biol Chem 279(45): 46692-46699.
Pavithra, S. R., R. Kumar and U. Tatu (2007). Systems analysis of chaperone networks in the malarial parasite *Plasmodium falciparum*. PLoS Comput Biol 3(9): 1701-1715.
Pesce, E. R., I. L. Cockburn, J. L. Goble, L. L. Stephens and G. L. Blatch (2010). Malaria heat shock proteins: drug targets that chaperone other drug targets. Infect Disord Drug Targets 10(3): 147-157.
Pham, T. V., S. R. Piersma, M. Warmoes and C. R. Jimenez (2010). On the beta-binomial model for analysis of spectral count data in label-free tandem mass spectrometry-based proteomics. Bioinformatics 26(3): 363-369.
Posfai, D., A. L. Eubanks, A. I. Keim, K. Y. Lu, G. Z. Wang, P. F. Hughes, N. Kato, T. A. Haystead and E. R. Derbyshire (2018). Identification of Hsp90 inhibitors with anti-Plasmodium activity. Antimicrob Agents Chemother.
Prince, H. M. and M. Dickinson (2012). Romidepsin for cutaneous T-cell lymphoma. Clin Cancer Res 18(13): 3509-3515.
Princeton University. "Generic Gene Ontology Term Mapper." Retrieved 20th December, 2017, from http://go.princeton.edu/cgi-bin/GOTermMapper.
RTS, S. C. T. P. (2015). Efficacy and safety of RTS,S/AS01 malaria vaccine with or without a booster dose in infants and children in Africa: final results of a phase 3, individually randomised, controlled trial. Lancet 386(9988): 31-45.
RTS, S. C. T. P., S. T. Agnandji, B. Lell, J. F. Fernandes, B. P. Abossolo, B. G. Methogo, A. L. Kabwende, A. A. Adegnika, B. Mordmuller, S. Issifou, P. G. Kremsner, J.

Sacarlal, P. Aide, M. Lanaspa, J. J. Aponte, S. Machevo, S. Acacio, H. Bulo, B. Sigauque, E. Macete, P. Alonso, S. Abdulla, N. Salim, R. Minja, M. Mpina, S. Ahmed, A. M. Ali, A. T. Mtoro, A. S. Hamad, P. Mutani, M. Tanner, H. Tinto, U. D'Alessandro, H. Sorgho, I. Valea, B. Bihoun, I. Guiraud, B. Kabore, O. Sombie, R. T. Guiguemde, J. B. Ouedraogo, M. J. Hamel, S. Kariuki, M. Oneko, C. Odero, K. Otieno, N. Awino, M. McMorrow, V. Muturi-Kioi, K. F. Laserson, L. Slutsker, W. Otieno, L. Otieno, N. Otsyula, S. Gondi, A. Otieno, V. Owira, E. Oguk, G. Odongo, J. B. Woods, B. Ogutu, P. Njuguna, R. Chilengi, P. Akoo, C. Kerubo, C. Maingi, T. Lang, A. Olotu, P. Bejon, K. Marsh, G. Mwambingu, S. Owusu-Agyei, K. P. Asante, K. Osei-Kwakye, O. Boahen, D. Dosoo, I. Asante, G. Adjei, E. Kwara, D. Chandramohan, B. Greenwood, J. Lusingu, S. Gesase, A. Malabeja, O. Abdul, C. Mahende, E. Liheluka, L. Malle, M. Lemnge, T. G. Theander, C. Drakeley, D. Ansong, T. Agbenyega, S. Adjei, H. O. Boateng, T. Rettig, J. Bawa, J. Sylverken, D. Sambian, A. Sarfo, A. Agyekum, F. Martinson, I. Hoffman, T. Mvalo, P. Kamthunzi, R. Nkomo, T. Tembo, G. Tegha, M. Tsidya, J. Kilembe, C. Chawinga, W. R. Ballou, J. Cohen, Y. Guerra, E. Jongert, D. Lapierre, A. Leach, M. Lievens, O. Ofori-Anyinam, A. Olivier, J. Vekemans, T. Carter, D. Kaslow, D. Leboulleux, C. Loucq, A. Radford, B. Savarese, D. Schellenberg, M. Sillman and P. Vansadia (2012). A phase 3 trial of RTS,S/AS01 malaria vaccine in African infants. N Engl J Med 367(24): 2284-2295.

RTS, S. C. T. P., S. T. Agnandji, B. Lell, S. S. Soulanoudjingar, J. F. Fernandes, B. P. Abossolo, C. Conzelmann, B. G. Methogo, Y. Doucka, A. Flamen, B. Mordmuller, S. Issifou, P. G. Kremsner, J. Sacarlal, P. Aide, M. Lanaspa, J. J. Aponte, A. Nhamuave, D. Quelhas, Q. Bassat, S. Mandjate, E. Macete, P. Alonso, S. Abdulla, N. Salim, O. Juma, M. Shomari, K. Shubis, F. Machera, A. S. Hamad, R. Minja, A. Mtoro, A. Sykes, S. Ahmed, A. M. Urassa, A. M. Ali, G. Mwangoka, M. Tanner, H. Tinto, U. D'Alessandro, H. Sorgho, I. Valea, M. C. Tahita, W. Kabore, S. Ouedraogo, Y. Sandrine, R. T. Guiguemde, J. B. Ouedraogo, M. J. Hamel, S. Kariuki, C. Odero, M. Oneko, K. Otieno, N. Awino, J. Omoto, J. Williamson, V. Muturi-Kioi, K. F. Laserson, L. Slutsker, W. Otieno, L. Otieno, O. Nekoye, S. Gondi, A. Otieno, B. Ogutu, R. Wasuna, V. Owira, D. Jones, A. A. Onyango, P. Njuguna, R. Chilengi, P. Akoo, C. Kerubo, J. Gitaka, C. Maingi, T. Lang, A. Olotu, B. Tsofa, P. Bejon, N. Peshu, K. Marsh, S. Owusu-Agyei, K. P. Asante, K. Osei-Kwakye, O. Boahen, S. Ayamba, K. Kayan, R. Owusu-Ofori, D. Dosoo, I. Asante, G. Adjei, G. Adjei, D. Chandramohan, B. Greenwood, J. Lusingu, S. Gesase, A. Malabeja, O. Abdul, H. Kilavo, C. Mahende, E. Liheluka, M. Lemnge, T. Theander, C. Drakeley, D. Ansong, T. Agbenyega, S. Adjei, H. O. Boateng, T. Rettig, J. Bawa, J. Sylverken, D. Sambian, A. Agyekum, L. Owusu, F. Martinson, I. Hoffman, T. Mvalo, P. Kamthunzi, R. Nkomo, A. Msika, A. Jumbe, N. Chome, D. Nyakuipa, J. Chintedza, W. R. Ballou, M. Bruls, J. Cohen, Y. Guerra, E. Jongert, D. Lapierre, A. Leach, M. Lievens, O. Ofori-Anyinam, J. Vekemans, T. Carter, D. Leboulleux, C. Loucq, A. Radford, B. Savarese, D. Schellenberg, M. Sillman and P. Vansadia (2011). First results of phase 3 trial of RTS,S/AS01 malaria vaccine in African children. N Engl J Med 365(20): 1863-1875.

Russo, I., S. Babbitt, V. Muralidharan, T. Butler, A. Oksman and D. E. Goldberg (2010). Plasmepsin V licenses *Plasmodium* proteins for export into the host erythrocyte. Nature 463(7281): 632-636.

Saksouk, N., M. M. Bhatti, S. Kieffer, A. T. Smith, K. Musset, J. Garin, W. J. Sullivan, Jr., M. F. Cesbron-Delauw and M. A. Hakimi (2005). Histone-modifying complexes regulate gene expression pertinent to the differentiation of the protozoan parasite Toxoplasma gondii. Mol Cell Biol 25(23): 10301-10314.

Searle, B. C. (2010). Scaffold: a bioinformatic tool for validating MS/MS-based proteomic studies. Proteomics 10(6): 1265-1269.
Sengupta, N. and E. Seto (2004). Regulation of histone deacetylase activities. J Cell Biochem 93(1): 57-67.
Sessler, N., K. Krug, A. Nordheim, B. Mordmuller and B. Macek (2012). Analysis of the *Plasmodium falciparum* proteasome using Blue Native PAGE and label-free quantitative mass spectrometry. Amino Acids 43(3): 1119-1129.
Shahbazian, M. D. and M. Grunstein (2007). Functions of site-specific histone acetylation and deacetylation. Annu Rev Biochem 76: 75-100.
Shi, Y., M. Dong, X. Hong, W. Zhang, J. Feng, J. Zhu, L. Yu, X. Ke, H. Huang, Z. Shen, Y. Fan, W. Li, X. Zhao, J. Qi, H. Huang, D. Zhou, Z. Ning and X. Lu (2015). Results from a multicenter, open-label, pivotal phase II study of chidamide in relapsed or refractory peripheral T-cell lymphoma. Ann Oncol 26(8): 1766-1771.
Shonhai, A. (2010). Plasmodial heat shock proteins: targets for chemotherapy. FEMS Immunol Med Microbiol 58(1): 61-74.
Thompson, C. A. (2014). Belinostat approved for use in treating rare lymphoma. Am J Health Syst Pharm 71(16): 1328.
Tonkin, C. J., C. K. Carret, M. T. Duraisingh, T. S. Voss, S. A. Ralph, M. Hommel, M. F. Duffy, L. M. Silva, A. Scherf, A. Ivens, T. P. Speed, J. G. Beeson and A. F. Cowman (2009). Sir2 paralogues cooperate to regulate virulence genes and antigenic variation in *Plasmodium falciparum*. PLoS Biol 7(4): e84.
UniProt, C. (2015). UniProt: a hub for protein information. Nucleic Acids Res 43(Database issue): D204-212.
Wang, T., W. H. Bisson, P. Maser, L. Scapozza and D. Picard (2014). Differences in conformational dynamics between Plasmodium falciparum and human Hsp90 orthologues enable the structure-based discovery of pathogen-selective inhibitors. J Med Chem 57(6): 2524-2535.
Wang, T., P. Maser and D. Picard (2016). Inhibition of Plasmodium falciparum Hsp90 Contributes to the Antimalarial Activities of Aminoalcohol-carbazoles. J Med Chem 59(13): 6344-6352.
WHO (2016). Global Malaria Programme: Artemisinin and artemisinin-based combination therapy resistance (Status Report).
WHO (2017). World Malaria Report 2017.
Yang, X. J. (2004). The diverse superfamily of lysine acetyltransferases and their roles in leukemia and other diseases. Nucleic Acids Res 32(3): 959-976.
Yoon, H. G., D. W. Chan, Z. Q. Huang, J. Li, J. D. Fondell, J. Qin and J. Wong (2003). Purification and functional characterization of the human N-CoR complex: the roles of HDAC3, TBL1 and TBLR1. EMBO J 22(6): 1336-1346.
Zininga, T., I. Achilonu, H. Hoppe, E. Prinsloo, H. W. Dirr and A. Shonhai (2016). *Plasmodium falciparum* Hsp70-z, an Hsp110 homologue, exhibits independent chaperone activity and interacts with Hsp70-1 in a nucleotide-dependent fashion. Cell Stress Chaperones 21(3): 499-513.
Zininga, T., C. P. Anokwuru, M. T. Sigidi, M. P. Tshisikhawe, I. I. D. Ramaite, A. N. Traore, H. Hoppe, A. Shonhai and N. Potgieter (2017). Extracts Obtained from Pterocarpus angolensis DC and Ziziphus mucronata Exhibit Antiplasmodial Activity and Inhibit Heat Shock Protein 70 (Hsp70) Function. Molecules 22(8).

Legends to Figures

Figure 1 Western blot analysis of immunoprecipitations using *P. falciparum* trophozoite protein lysates and anti-*Pf*HDAC1 antibody. (A*i-iv*) Representative microscopic images of Quick Dip-stained *P. falciparum* 3D7 trophozoite stage parasites that were used to prepare four independent protein lysates for immunoprecipitation. **(B)** Immunoprecipitation was performed using synchronous trophozoite-stage *P. falciparum* 3D7 lysates (*Pf*3D7; panels **B*i*-B*iv***) using anti-*Pf*HDAC1 antibody followed by Western blot analysis using the same anti-*Pf*HDAC1 antibody. Each independent experiment included the starting material (**SM**), wash 3 (**W3**; wash 1 and 2 not shown) and eluate (**E**) for the ***Pf*3D7** test sample and control samples. Controls included a protein negative (PBS only) control (**PROT-NEG**), antibody negative control (**AB-NEG**) and a red blood cell control (**RBC**).

Figure 2 Volcano plot displaying the estimated $\log_2$ fold-changes for *Pf*3D7 eluate versus AB-NEG eluate control immunoprecipitation versus the -$\log_{10}$ beta-binomial P-values for 135 quantified proteins. Candidate *Pf*HDAC1 complex proteins (i.e. proteins with a P-value < 0.01 and greater than two-fold difference) are highlighted in red. *Pf*HDAC1 and proteins selected for validation experiments (*Pf*Hsp70-1 and *Pf*Hsp90) are labelled.

Figure 3 Annotated gene ontology (GO) biological processes for 26 candidate *Pf*HDAC1 interacting proteins identified using immunoprecipitation and mass spectrometry. Annotated GO biological processes were downloaded from PlasmoDB. Multiple GO terms for individual genes are included.

Figure 4 Protein complex co-localisation analysis of *Pf*HDAC1 in *P. falciparum* asexual intraerythrocytic lifecycle stages using BN PAGE and Western blot. Asexual intraerythrocytic *P. falciparum* 3D7 samples (**ER**, early rings; **LR/ET**, late rings/early trophozoites; **LT**, late trophozoites; **S/ER/LT**, schizont/early rings/late trophozoites) were

analysed by 3-12% BN PAGE followed by Western blot using anti-*Pf*HDAC1 antibody (**A-B**), anti-*Pf*Hsp70-1 antibody (**A, C**) and anti-*Pf*Hsp90 antibody (**B, C**), all on the same membrane. The membrane was stripped in between each probe and complete stripping confirmed by imaging on a VersaDoc 4000MP imaging system (Bio-Rad, USA). Image J 1.51d software was used to overlay Western blot images to determine co-localisation of *Pf*HDAC1 and complex proteins (**Merge**).

Figure 5 Two dimensional BN PAGE / SDS PAGE analysis of *P. falciparum* protein lysates. Protein lysate was prepared from synchronous *P. falciparum* trophozoite stage parasites, followed by 3-12% BN PAGE. The BN PAGE lane (**A**) was excised and protein complexes separated in a second dimension with 10% SDS PAGE, followed by either colloidal Coomassie blue staining (**B**) or two-colour Western blot analysis (**C**). The PVDF membrane was first probed with anti-*Pf*HDAC1 antibody and anti-IRDye 680RD goat anti-rabbit secondary antibody (red) and then re-probed with anti-*Pf*Hsp70-1 antibody and anti-IRDye 800CW goat anti-rabbit secondary antibody (green). Panel ***i*** and ***ii*** (dashed boxes) highlight complexes in which both *Pf*HDAC1 and *Pf*Hsp70-1 were identified.

775 **Table 1 *P. falciparum* proteins significantly enriched in immunoprecipitations with anti-*Pf*HDAC1 antibody (P < 0.01 and greater than**

776 **two-fold difference).**

#	Annotated Protein Name[a]	PlasmoDB ID[a]	~kDa	P-value[b]	Log_2 fold-change
1	heat shock protein 70	PF3D7_0818900	74	2.13E-05	1.62
2	heat shock protein 110	PF3D7_0708800	100	2.89E-05	2.52
3	histone deacetylase 1	PF3D7_0925700	51	7.07E-05	2.75
4	tubulin binding cofactor c, putative	PF3D7_1015700	39	8.49E-05	2.24
5	haloacid dehalogenase-like hydrolase, putative	PF3D7_1226300	33	0.000118	2.09
6	DNA replication licensing factor MCM2	PF3D7_1417800	112	0.000394	1.91
7	60S ribosomal protein L4	PF3D7_0507100	46	0.000464	1.70
8	40S ribosomal protein S5	PF3D7_1447000	30	0.000506	1.89
9	26S protease regulatory subunit 6A, putative	PF3D7_1130400	50	0.000796	2.17
10	pyruvate kinase	PF3D7_0626800	56	0.00082	2.12
11	heat shock protein 90	PF3D7_0708400	86	0.001418	1.10
12	conserved *Plasmodium* protein, unknown function	PF3D7_1120000	129	0.001445	1.70

13	60S ribosomal protein P0	PF3D7_1130200	35	0.002007	1.58
14	asparagine--tRNA ligase	PF3D7_0211800	71	0.002024	1.02
15	60S ribosomal protein L3	PF3D7_1027800	44	0.002506	1.78
16	heat shock protein 60	PF3D7_1015600	63	0.002521	1.70
17	40S ribosomal protein S17, putative	PF3D7_1242700	16	0.003512	1.43
18	exported protein 1	PF3D7_1121600	17	0.004249	1.49
19	V-type proton ATPase subunit B	PF3D7_0406100	56	0.004553	1.68
20	phosphoglycerate kinase	PF3D7_092250	45	0.005007	1.80
21	40S ribosomal protein S11, putative	PF3D7_0317600	19	0.005273	1.69
22	40S ribosomal protein S11	PF3D7_0516200	16	0.005301	1.50
23	elongation factor 2	PF3D7_1451100	94	0.005478	1.58
24	proliferation-associated protein 2g4, putative	PF3D7_1428300	43	0.007116	1.38
25	14-3-3 protein	PF3D7_0818200	30	0.007244	1.39
26	60S acidic ribosomal protein P2	PF3D7_0309600	12	0.008323	1.32
27	60S ribosomal protein L34	PF3D7_0710600	17	0.009483	1.17

777 [a](Aurrecoechea et al. 2009); [b]P-value estimated using a beta-binomial test (Pham et al. 2010).

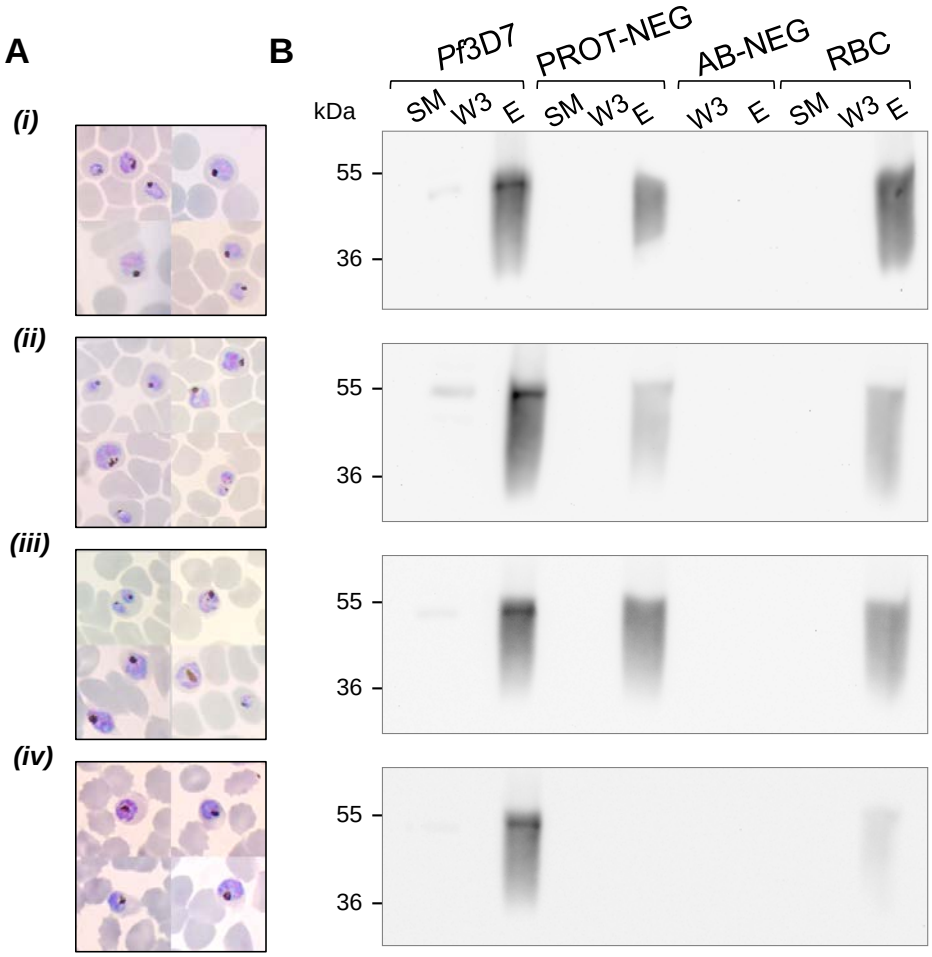
A
(i)
(ii)
(iii)
(iv)
B
Pf3D7
PROT-NEG
AB-NEG
RBC
kDa
SM
W3
E
55
36

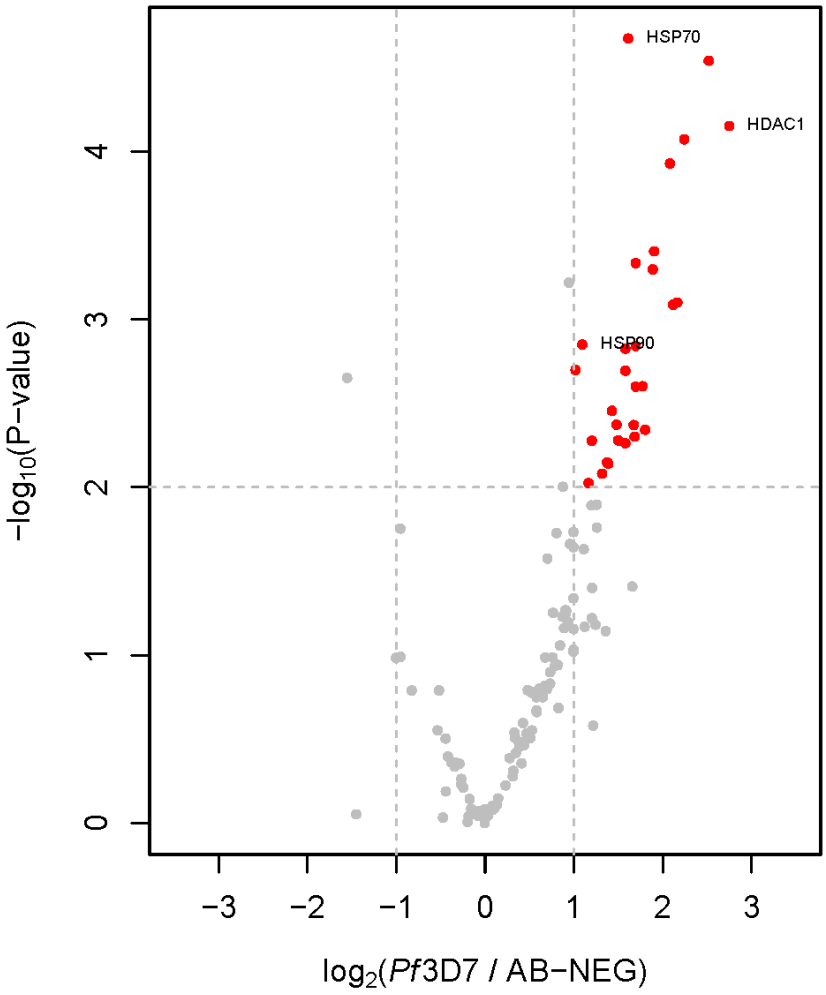
HSP70
HDAC1
HSP90
−log10(P−value)
log2(Pf3D7 / AB−NEG)
0
1
2
3
4
−3
−2
−1
0
1
2
3

Biological Processes

0 2 4 6 8

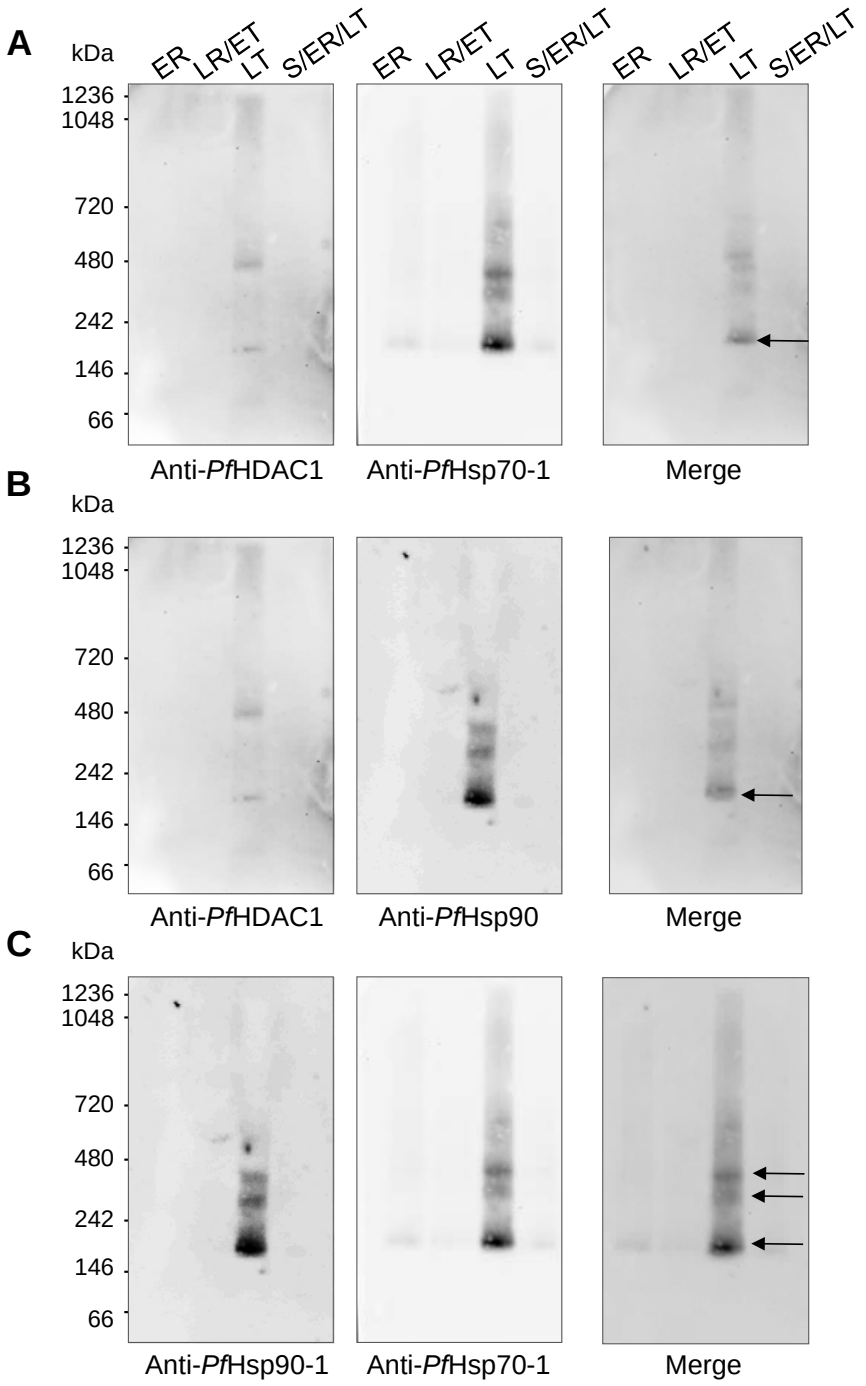
A
kDa
ER
LR/ET
LT
S/ER/LT
1236
1048
720
480
242
146
66
Anti-PfHDAC1
Anti-PfHsp70-1
Merge
B
Anti-PfHDAC1
Anti-PfHsp90
Merge
C
Anti-PfHsp90-1
Anti-PfHsp70-1
Merge

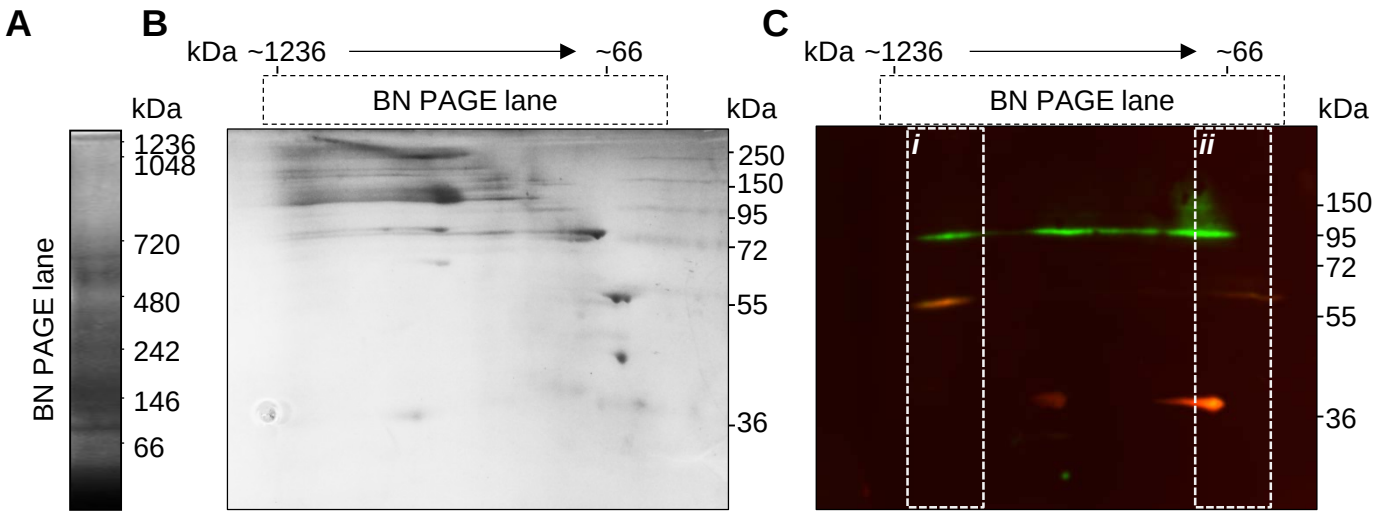
A
B
C
kDa
1236
1048
720
480
242
146
66
BN PAGE lane
kDa ~1236
~66
BN PAGE lane
kDa
250
150
95
72
55
36
kDa ~1236
~66
BN PAGE lane
kDa
i
ii
150
95
72
55
36

Supplementary Table 1 GO Term Mapper (Biological Process)[1].

GO Biological Process	Protein PlasmoDB Accession #
cellular nitrogen compound metabolic process (GO:0034641)	PF3D7_0211800, PF3D7_0309600, PF3D7_0317600, PF3D7_0507100, PF3D7_0516200, PF3D7_0626800, PF3D7_1027800, PF3D7_1121600, PF3D7_1130200, PF3D7_1242700, PF3D7_1417800, PF3D7_1447000, PF3D7_1451100
biosynthetic process (GO:0009058)	PF3D7_0211800, PF3D7_0309600, PF3D7_0317600, PF3D7_0507100, PF3D7_0516200, PF3D7_1027800, PF3D7_1130200, PF3D7_1242700, PF3D7_1417800, PF3D7_1447000, PF3D7_1451100
translation (GO:0006412)	PF3D7_0211800, PF3D7_0309600, PF3D7_0317600, PF3D7_0507100, PF3D7_0516200, PF3D7_1027800, PF3D7_1130200, PF3D7_1242700, PF3D7_1447000, PF3D7_1451100
response to stress (GO:0006950)	PF3D7_0708400, PF3D7_0818900, PF3D7_1015600
small molecule metabolic process (GO:0044281)	PF3D7_0211800, PF3D7_0626800
cofactor metabolic process (GO:0051186)	PF3D7_0626800, PF3D7_1121600
cell cycle (GO:0007049)	PF3D7_1417800, PF3D7_1428300
sulfur compound metabolic process (GO:0006790)	PF3D7_1121600
DNA metabolic process (GO:0006259)	PF3D7_1417800
symbiosis, encompassing mutualism through parasitism (GO:0044403)	PF3D7_0309600
cell proliferation (GO:0008283)	PF3D7_1428300
carbohydrate metabolic process (GO:0005975)	PF3D7_0626800
protein folding (GO:0006457)	PF3D7_1015600
protein targeting (GO:0006605)	PF3D7_1015600
transport (GO:0006810)	PF3D7_1015600
homeostatic process GO:0042592)	PF3D7_0406100
cellular amino acid metabolic process (GO:0006520)	PF3D7_0211800
tRNA metabolic process (GO:0006399)	PF3D7_0211800
generation of precursor metabolites and energy (GO:0006091)	PF3D7_0626800
cellular component assembly (GO:0022607)	PF3D7_0626800
macromolecular complex assembly (GO:0065003)	PF3D7_0626800
mitochondrion organization (GO:0007005)	PF3D7_1015600
catabolic process (GO:0009056)	PF3D7_0626800
protein complex assembly (GO:0006461)	PF3D7_0626800

[1] http://go.princeton.edu/cgi-bin/GOTermMapper

Supplementary Table 2 GO Term Mapper (Function)[1].

GO Function	Protein PlasmoDB Accession #
structural molecule activity (GO:0005198)	PF3D7_0317600, PF3D7_0507100, PF3D7_1027800, PF3D7_1130200, PF3D7_1242700, PF3D7_1447000
structural constituent of ribosome (GO:0003735)	PF3D7_0317600, PF3D7_0507100, PF3D7_1027800, PF3D7_1130200, PF3D7_1242700, PF3D7_1447000
ATPase activity (GO:0016887)	PF3D7_0406100, PF3D7_0708400, PF3D7_1015600, PF3D7_1130400
RNA binding (GO:0003723)	PF3D7_0516200, PF3D7_1451100
peptidase activity (GO:0008233)	PF3D7_1130400, PF3D7_1428300
histone binding (GO:0042393)	PF3D7_0818200
translation factor activity, RNA binding (GO:0008135)	PF3D7_1451100
ion binding (GO:0043167)	PF3D7_1451100
ligase activity (GO:0016874)	PF3D7_0211800
transferase activity, transferring alkyl or aryl (other than methyl) groups (GO:0016765)	PF3D7_1121600
transmembrane transporter activity (GO:0022857)	PF3D7_0406100

[1] http://go.princeton.edu/cgi-bin/GOTermMapper

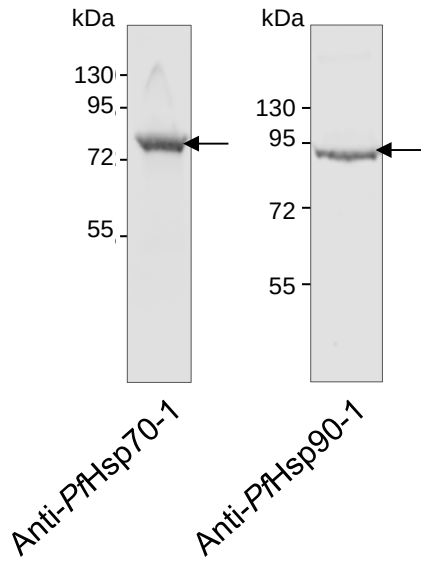

Supplementary Figure 1 Western blots of *P. falciparum* protein lysates. Synchronous trophozoite-stage *P. falciparum* parasite protein lysate was separated by SDS PAGE and Western blot analysis carried out using either anti-*Pf*Hsp70-1 (1:2000 dilution) or anti-*Pf*Hsp90-1 (1:2000 dilution). Anti-rabbit HRP (1:2000 dilution) was used as the secondary antibody and membranes imaged on a VersaDoc 4000MP imaging system.

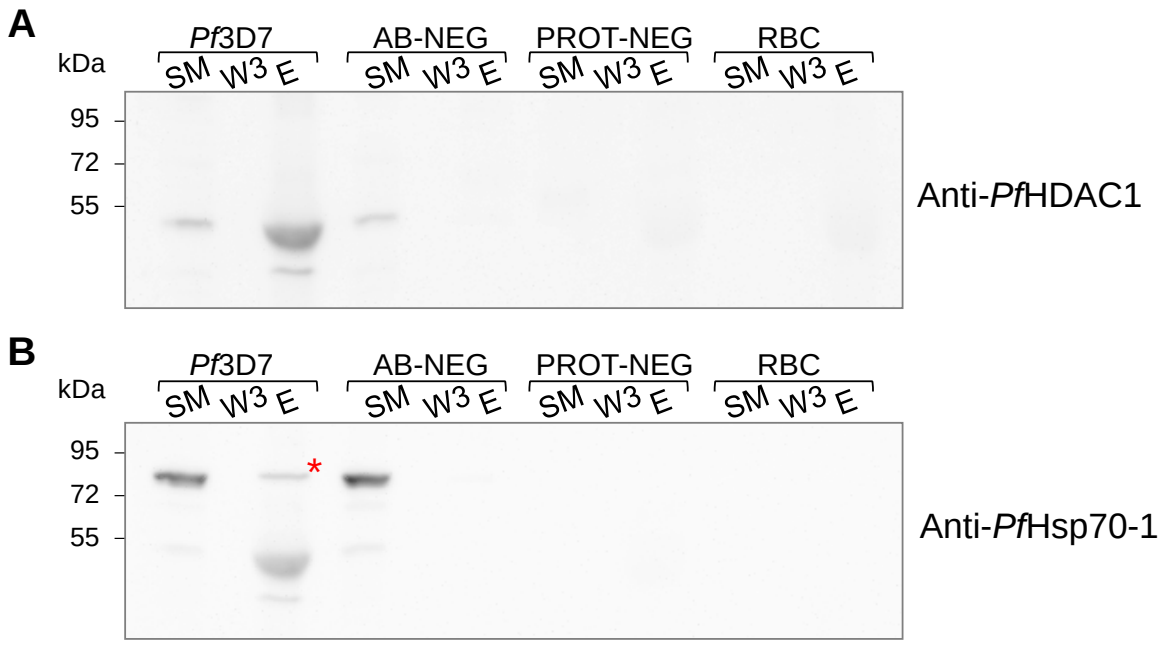

Supplementary Figure 2 Western blots showing co-immunoprecipitation of *Pf*HDAC1 and *Pf*Hsp70-1 using anti-*Pf*HDAC1 antibody. Western blot of *P. falciparum* trophozoite-stage protein eluate following immunoprecipitation using anti-*Pf*HDAC1 antibody. **(A)** A band the expected size of *Pf*HDAC1 (~51 kDa) was detected in the starting material (SM) of the *Pf*3D7 and AB-NEG samples and in the *Pf*3D7 eluate, using anti-*Pf*HDAC1 antibody. The lower molecular weight band is likely cross reactivity due to enrichment of the eluate sample. **(B)** The same PVDF membrane was re-probed (without stripping) with anti-*Pf*Hsp70-1 antibody. A band the expected size of *Pf*Hsp70-1 (~74 kDa) was detected in the SM of the *Pf*3D7 and AB-NEG samples, and in the *Pf*3D7 eluate. **SM,** starting material; **W3,** wash 3; **E**, eluate; ***Pf*3D7**, *P. falciparum* 3D7 trophozoite protein lysate; **AB-NEG**, antibody negative control; **PROT-NEG**, protein negative control; **RBC**, red blood cell control.

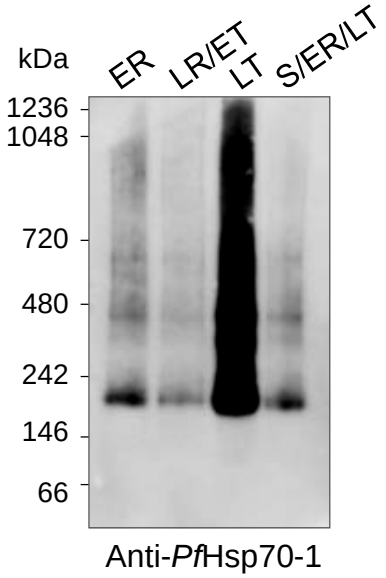

Supplementary Figure 3 *P. falciparum* intraerythrocytic lifecycle stage BN PAGE and Western blot analysis using anti-*Pf*Hsp70-1 antibody. The PVDF membrane has been overexposed to show protein complexes recognised by anti-*Pf*Hsp70-1 antibody in the early ring (**ER**), late ring/early trophozoite (**LR/ET**) and schizont/early ring/late trophozoite (**S/ER/LT**) protein lysate preparations. The same blot is shown in Figure 4 of the primary manuscript.